

Bilateral transactions impact voltage stability and nodal pricing in power networks

Ganesh Wakte¹, Mukesh Kumar², Mohammad Aljaidi³, Ramesh Kumar⁴, Manish Kumar Singla⁵

¹Department of Electrical Engineering, Faculty of Engineering, Tulsiramji Gaikwad Patil College of Engineering and Technology, Nagpur, India

²Department of Electrical Engineering, Faculty of Engineering, G H Raisoni University, Amravati, India

³Department of Computer Science, Faculty of Information Technology, Zarqa University, Zarqa, Jordan

⁴Department of Electrical Engineering, Faculty of Engineering, Chitkara University Institute of Engineering and Technology, Chitkara University, Rajpura, India

⁵Department of Biosciences, Faculty of Science, Saveetha School of Engineering, Saveetha Institute of Medical and Technical Sciences, Chennai, India

Article Info

Article history:

Received Nov 10, 2024

Revised Sep 30, 2025

Accepted Oct 14, 2025

Keywords:

Bilateral transactions

High voltage direct current

Megavolt-ampere-mile

Megawatt-mile

Nodal pricing

Optimal power flow

Voltage stability

ABSTRACT

This study investigates the impact of bilateral transactions on voltage stability and nodal pricing in the Indian power grid using a modified IEEE 30-bus system. A high voltage direct current (HVDC) link is integrated into the network to enhance control and system flexibility. Two advanced transmission pricing mechanisms—megawatt (MW)-Mile and megavolt-ampere (MVA)-Mile—are employed to allocate costs based on power flow magnitude and distance. The analysis incorporates hybrid AC-DC optimal power flow (OPF) modeling under various transaction levels. Simulation results show that a 100 MW bilateral transaction reduces the voltage at the receiving bus (bus 28) by 2% (from 1.05 to 1.03 p.u.) and increases the nodal price by 6.25% (from ₹4.80 to ₹5.10/kWh). The use of HVDC technology reduces total generation cost by approximately 8.2% (from ₹85 lakhs to ₹78 lakhs) and decreases real power loss from 70 MW to 50 MW. These findings confirm that bilateral transactions influence voltage profiles and market pricing. Moreover, MW-Mile and MVA-Mile methods demonstrate effective cost allocation capabilities. The proposed approach offers a practical framework for improving grid reliability and economic transparency in evolving power markets.

This is an open access article under the [CC BY-SA](#) license.



Corresponding Author:

Ganesh Wakte

Department of Electrical Engineering, Faculty of Engineering

Tulsiramji Gaikwad Patil College of Engineering and Technology

Nagpur, Maharashtra, India

Email: ganeshwakte1989@gmail.com

1. INTRODUCTION

The past two decades have witnessed significant restructuring in electricity markets globally. This restructuring aims to introduce competition in the bulk power and retail segments of the electric power industry, enhancing economic efficiency and encouraging private investment [1]. While the primary motivation for restructuring in economically advanced regions has been to improve overall efficiency, in rapidly growing economies like China and India, the focus has been on attracting private investment to support the expansion of the electric sector, thus alleviating the financial burden on governments [2].

Separation of generation and transmission services, allowing for the transmission network to be accessed by all participants of the eligible market under an open-access system, is a key aspect of this

restructuring. This shift has significantly changed the landscape of the power industry, introducing fresh challenges in generation, transmission, and system operation [3]. The competitive nature of the modern electric power industry requires new strategies to enhance both the economic performance and the reliability of power systems [4].

In this context, the present study sets out with four primary objectives. First, it aims to analyze the motivations behind electricity transmission pricing, focusing on economic and regulatory drivers that influence market efficiency and competition. Second, the study develops and validates advanced pricing methodologies using sophisticated hybrid AC-DC optimal power flow (OPF) models [5], [6]. Third, it applies these methodologies to both a real-world modified IEEE 30-bus system and a simplified five-bus configuration to compute transmission prices and assess practical implementation. Finally, the study evaluates the suitability of megawatt (MW)-Mile and megavolt-ampere (MVA)-Mile pricing mechanisms for developing countries like India, considering their unique challenges in infrastructure, regulation, and market operations [7], [8].

These objectives are pursued through comprehensive modeling, including high voltage direct current (HVDC) integration and bilateral transaction scenarios, with a focus on analyzing voltage stability and nodal pricing under varying load conditions [9]. The use of hybrid OPF and dynamic pricing structures aims to offer actionable insights for more transparent and efficient cost allocation in modern transmission networks [10].

2. LITERATURE REVIEW

The liberalization of electricity markets has accelerated the adoption of bilateral transactions, wherein participants negotiate power exchanges independently of centralized clearing mechanisms. These market structures aim to improve flexibility, efficiency, and cost reflectiveness in both developed and developing countries. Yi *et al.* [11] proposed a fuzzy Nash bargaining framework for bilateral trades, enhancing negotiation outcomes while accounting for uncertainty. Kong *et al.* [12] modeled bilateral contracts using Bayesian game theory, illustrating strategic behavior in competitive power markets. Lingcheng *et al.* [13] investigated the integration of service differentiation into bilateral platforms, emphasizing the importance of competitive strategies and platform-based governance in emerging electricity economies.

In India's evolving deregulated market, bilateral transactions have seen exponential growth under open-access provisions. Algarvio [14] developed an agent-based local energy trading model and observed that bilateral transactions may challenge transmission corridors and voltage stability, particularly during peak demand.

To accommodate increased bilateral trades and intermittent renewables, HVDC and, particularly, voltage source converter-high voltage direct current (VSC-HVDC) systems are being integrated to provide controllability and voltage support. Lu *et al.* [15] conducted a stability assessment of grid-forming VSC-HVDC systems and developed control strategies to mitigate instability under weak-grid scenarios. Similarly, researchers studied power optimization controls that effectively suppress frequency oscillations using VSC-HVDC links. Renedo *et al.* [16] showed that coordinated multi-terminal HVDC control enhances transient stability during system disturbances. Singh *et al.* [17] emphasized the role of VSC-based fast frequency response in damping oscillations, especially in hybrid AC/DC networks.

Advancements in internal voltage control have improved converter resilience. Wu and Wang [18] introduced adaptive dual-timescale control for grid-forming VSCs, offering robustness under varying system inertia. Rashmi and Gaonkar [19] further streamlined VSC-HVDC modeling for multi-machine grids, aiding simulation of dynamic events under real-time constraints.

Transmission pricing methods have increasingly moved toward frameworks that better reflect actual network usage and the spatial character of grid services. Traditional embedded approaches—such as the Postage Stamp method—allocate transmission cost uniformly and therefore fail to reflect locational or flow-based usage of the network. To overcome these limitations, flow-based cost-allocation methods such as the MW-Mile and MVA-Mile approaches allocate charges in proportion to power flows multiplied by distance or network usage, thereby linking cost responsibility more directly to the utilization of transmission assets. For example, Andukury and Sarada [20] demonstrate how the MW-Mile method, based on active-power flows and line lengths, provides a more usage-sensitive allocation of fixed transmission costs. Further, Yang [21] proposes an objective transmission cost allocation method based on marginal usage and shows how MW-Mile constructs may be embedded within marginal-cost frameworks.

Beyond pure flow-distance methods, newer work incorporates marginal-benefit or marginal-cost concepts in transmission pricing. Liu *et al.* [22] develop a transmission price design that divides costs into an “expansion cost” component (derived from marginal benefits of the transmission network) and a residual cost allocated in a usage-reflective way, thereby integrating spatial and temporal demand information into pricing. At the same time, the principle of “beneficiaries pay” in transmission cost-allocation is emphasized by Hogan [23], who argues that efficient cost-allocation should reflect both marginal cost signals and usage/benefit

attribution. Finally, loss-based and distance-sensitive cost drivers are addressed by Eldridge *et al.* [24], who examine marginal loss pricing and demonstrate how loss-sensitive allocation affects nodal pricing and transmission cost recovery; and Jing *et al.* [25] review a variety of cost allocation schemes (including MW-Mile, Shapley value, and nucleolus methods) and highlight their comparative advantages and limitations in fair, usage-based cost allocation frameworks.

These evolving pricing models, coupled with HVDC flexibility, provide foundational tools for reliable bilateral trading in meshed networks. Their relevance to India's regulatory goals under general network access (GNA) highlights the practical feasibility of implementing MW-Mile and VSC-HVDC-based solutions for a fair and resilient power system.

3. METHOD

Electricity transmission pricing is shaped by both economic and regulatory imperatives, crucial for establishing effective pricing frameworks that enhance market efficiency, ensure cost recovery, and promote competition [6]. Figure 1 shows the flow diagram of the system in this study.

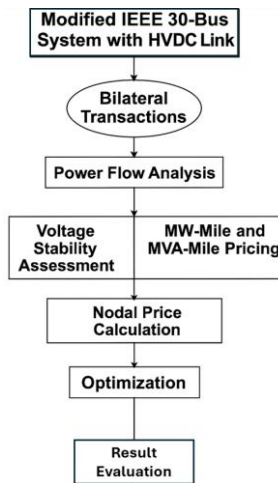


Figure 1. Flowchart of the system

3.1. System description

Developing transmission pricing methodologies using hybrid AC-DC OPF models involves several mathematical and computational steps. This section outlines the process of deriving embedded and nodal pricing from the OPF model [26].

The test power system used for simulation comprises five buses interconnected by transmission lines, with an HVDC link between bus 1 and bus 5. Each bus is equipped with generators characterized by their capacities, operational constraints (both lower and upper bounds on power output), and fuel cost functions expressed in dollars per megawatt-hour (\$/MWh). Table 1 provides a detailed overview of the generator data used for simulation.

Table 1. Generator data and characteristics

Bus	Generator capacity (MW)	Lower bound (MW)	Upper bound (MW)	Fuel cost function (\$/MWh)
1	150	50	200	$f_1 = 5P_{G1} + 0.1P_{G1}^2$
2	200	80	250	$f_1 = 6P_{G2} + 0.12P_{G2}^2$
3	180	60	220	$f_1 = 5.5P_{G3} + 0.11P_{G3}^2$
4	250	100	300	$f_1 = 7P_{G4} + 0.15P_{G4}^2$
5	300	120	350	$f_1 = 8P_{G5} + 0.16P_{G5}^2$

3.1.1. Model of AC-DC optimal power flow formulation

The hybrid model for AC-DC OPF is formulated to minimize the operational cost within the power system while satisfying various physical and operational constraints. The mathematical formulation includes: the objective function, which represents short-term operating costs like fuel expenses, can be expressed as (1) [27]:

$$\text{Minimize } f(X, P, Q) = \sum_{i=1}^{NG} (a_i P_{Gi}^2 + b_i P_{Gi} + c_i) \quad (1)$$

where X denotes the state variables vector (for imaginary and real voltages of bus), P and Q denote the vectors of reactive as well as active power demands for each bus, respectively, and a_i, b_i, c_i denotes cost coefficients for i^{th} generator.

Equality constraints depict equations of power-flow balance, ensuring that the total generated power matches the combined power demands and losses throughout the network [28]:

$$S(X, P, Q) = 0 \text{ Or } P_G + P_D + P_{DC} + P_L \text{ and } Q_G = Q_D + Q_{DC} + Q_L \quad (2)$$

where P_G and Q_G are the total generated reactive and active power, P_D and Q_D are the demanded active and the reactive power, P_{DC} and Q_{DC} denotes active and the reactive power at the DC terminals, and P_L and Q_L are the transmission losses.

3.1.2. High voltage direct current system modelling and integration

The HVDC system integrated into this study is modeled to accurately represent the dynamics of power flow between AC and DC systems.

HVDC power flow equations: the DC power balance at each terminal. The corresponding AC side power injections are:

Active power:

$$P_{aci} = V_i I_{di} \cos(\alpha_i) \quad (3)$$

Reactive power:

$$Q_{aci} = V_i I_{di} \sin(\alpha_i) \quad (4)$$

where: V_i is the AC bus voltage and α_i is the converter firing/extinction angle.

Control strategies: the HVDC system operates under two common control modes: constant power control (rectifier mode) controls the DC power output by adjusting α_i . constant voltage control (inverter mode) regulates DC voltage to maintain system stability. The typical operational limits enforced in the model are:

$$\begin{aligned} \alpha_{min} &\leq \alpha_i \leq \alpha_{max} \\ V_{di}^{min} &\leq V_{di} \leq V_{di}^{max} \\ I_{di}^{max} &\leq I_{di} \leq I_{di}^{max} \end{aligned} \quad (5)$$

These constraints ensure safe and reliable operation of the HVDC link.

Embedding into AC-DC OPF: the AC-DC OPF incorporates the HVDC link as additional equality and inequality constraints. The power balance equations at buses connected to HVDC terminals are modified as (6):

$$\begin{aligned} P_{Gi} - P_{Di} - P_{aci} &= 0 \\ Q_{Gi} - Q_{Di} - Q_{aci} &= 0 \end{aligned} \quad (6)$$

The HVDC line loss can also be included as (7):

$$P_{loss} = R_{dc} I_{di}^2 \quad (7)$$

where R_{dc} is the DC line resistance.

3.2. Cost calculation approaches

3.2.1. Voltage stability metrics

Voltage stability is assessed using the L-Index method, which is a reliable indicator of proximity to voltage collapse. For a system with n buses, the L-Index for buses i is given by:

$$L_i = 1 - \sum_{j \in G} F_{ij} \frac{V_j}{V_i} e^{j(\delta_j - \delta_i)} \quad (8)$$

where: V_i and V_j are the voltages at the load bus i and generator bus j , δ_i , and δ_j are their voltage angles, and F_{ij} are elements of the matrix derived from the system's admittance matrix. A value of L_i approaching 1 indicates instability.

Alternatively, Jacobian-based indicators assess system solvability. The smallest singular value σ_{min} of the Jacobian matrix J from the power flow equations:

$$J = \frac{\partial(P, Q)}{\partial(\theta, V)} \quad (9)$$

is used to measure the distance to voltage collapse; a lower σ_{min} signals reduced stability margin.

3.2.2. MW-Mile pricing formulation

The MW-Mile method calculates the cost of transmission based on both power flow and distance. For a transaction T over line f , the allocated cost $C_{T,f}$ is:

$$C_{T,f} = \Delta P_f \times D_f \times R \quad (10)$$

where: ΔP_f is the change in active power (MW) on line f , due to the transaction, D_f is the length of the line (miles or km), and R is the rate per MW-Mile.

The total cost is the summation over all lines:

$$C_T = \sum_f C_{T,f} \quad (11)$$

3.2.3. MVA-Mile pricing formulation

The MVA-Mile method extends MW-Mile by including reactive power, using the line's apparent power S_f :

$$S_f = \sqrt{(P_f)^2 + (Q_f)^2} \quad (12)$$

The allocated cost per transaction is:

$$C_{T,f} = \Delta S_f \times D_f \times R \quad (13)$$

where ΔS_f is the change in MVA flow due to the transaction.

3.2.4. Nodal pricing formulation

Nodal pricing is derived from the Lagrangian of the OPF problem. For a system with equality constraints $g(x) = 0$ and inequality constraints $h(x) \leq 0$, the Lagrangian is:

$$L(x, \lambda, \mu) = f(x) + \lambda^T g(x) + \mu^T h(x) \quad (14)$$

The nodal price λ_i at bus i is the Lagrange multiplier associated with the active power balance at that node:

$$\lambda_i = \frac{\partial L}{\partial P_{Gi}} \quad (15)$$

it reflects the marginal cost of supplying an additional MW at the bus i , considering generation cost, congestion, and losses.

3.2.5. Integration in AC-DC optimal power flow

For combined AC-DC networks, additional terms model the HVDC link: active power at the DC converter bus i :

$$P_{di} = V_i I_{di} \cos(\alpha_i) \quad (16)$$

Reactive power:

$$Q_{di} = V_i I_{di} \sin(\alpha_i) \quad (17)$$

where α_i is the firing angle. These are included in the equality constraints for power balance.

3.3. Simulation steps

The implementation of the AC-DC OPF-based locational (nodal) pricing and embedded models is executed using MATLAB, leveraging its optimization toolbox and powerful scripting capabilities. The process begins with setting up the test power system within MATLAB, defining bus configurations, generator characteristics, including capacities and operational constraints, and demand profiles [16]. MATLAB's *fmincon* solver is then employed to formulate and solve the problem of AC-DC OPF, which aims to minimize the total generation costs subject to various constraints. These constraints typically include power balance equations, voltage limits at each bus (maintained between 0.95 and 1.05 per unit), and thermal limits on transmission lines.

This IEEE 30-bus configuration is widely acknowledged in power system research for its balanced complexity and size, making it ideal for validating methodologies and models. In this study, the standard configuration has been altered to more accurately represent real-world conditions and incorporate advanced technologies. The adjustments include adding HVDC links to enhance network flexibility and stability, updating load and generation profiles to simulate dynamic scenarios with varying demands and renewable energy sources, and incorporating bilateral transactions between buses to examine their effects on voltage stability and nodal pricing.

4. OPTIMIZATION

The AC-DC OPF model implemented in MATLAB's *fmincon* solver is designed to minimize total generation costs while adhering to stringent operational constraints and meeting demand requirements. This optimization task revolves around minimizing the aggregate operating expenses of generators, encompassing fuel costs and other operational charges. Key constraints addressed include maintaining power balance throughout the grid to ensure that total power supplied equals demand plus losses. Voltage limits are enforced to prevent bus voltages from exceeding predefined thresholds, safeguarding equipment and ensuring system stability. Additionally, thermal limits on transmission lines are imposed to prevent overloading, which could lead to overheating and potential damage.

Upon successful execution of the AC-DC OPF formulation, MATLAB provides comprehensive outputs. These outputs include optimized schedules for generator dispatch, flow allocations for HVDC links, and the total operational cost incurred by the system. Post-solution analysis involves scrutinizing bus voltage profiles, assessing the distribution of power flows across the network, and evaluating nodal prices at different buses under various transaction scenarios. This detailed analysis not only ensures optimal utilization of resources but also enhances the understanding of grid performance and economic implications associated with electricity transmission.

The optimization process within the Indian electricity grid focuses on achieving multiple objectives critical for enhancing economic efficiency, grid stability, and reliable power supply. One of the primary objectives is to minimize total generation costs while concurrently reducing reactive power, minimizing real power losses, and mitigating voltage deviations across the network. Achieving a significant reduction in total generation costs from 85,00,000 INR to 78,00,000 INR demonstrates the economic benefits of optimizing dispatch strategies, as given in Table 2. This reduction ensures more cost-effective utilization of generation resources across the grid, contributing to overall economic efficiency.

Table 2. Optimization results (Indian grid scenario)

Parameter	Without optimization	With optimization
Total generation cost (INR)	85,00,000	78,00,000
Total real power loss (MW)	70	50
Total reactive power (MVAR)	400	320
Voltage deviation (PU)	0.04	0.02

The optimization effort successfully decreases total reactive power from 400 MVAR to 320 MVAR. This reduction is crucial as it enhances voltage stability and reduces the reactive power burden on the grid, thereby improving operational efficiency and reliability. Real power losses are also significantly reduced from 70 MW to 50 MW through optimization. This reduction signifies enhanced transmission efficiency, minimized energy wastage, and strengthened energy conservation efforts within the grid infrastructure. Optimization leads to a decrease in voltage deviation from 0.04 PU to 0.02 PU. This improvement demonstrates more precise management of voltage levels, ensuring a stable and reliable electricity supply to consumers and industries.

5. ANALYSIS AND DISCUSSION

5.1. Simulation data

These parameters include the upper and lower bounds of power generation for each generator as well as the coefficients of their cost functions. The cost function is generally expressed as a quadratic function of the form [29]:

$$C(P) = aP^2 + bP + c \quad (18)$$

where P is the power output.

In the OPF analysis, these generators were dispatched to fulfill the load demand while minimizing the overall generation cost. The results of this optimization process were then used to assess the impact of different transmission pricing models on nodal prices and system efficiency given in Table 3.

Table 3. Generator parameters and costs

Generator	Lower bound (MW)	Upper bound (MW)	Cost function (a)	Cost function (b)	Cost function (c)
G1	10	80	0.02	10.0	500
G2	20	90	0.017	12.0	450
G13	15	85	0.025	11.0	470
G22	25	100	0.03	9.0	520
G23	20	95	0.028	10.5	480
G27	10	75	0.022	11.5	490

The Postage Stamp model might lead to higher nodal prices for some users who do not heavily utilize the transmission network, while the MW-Mile and MVA-Mile models would provide a more equitable distribution of costs based on actual usage. This detailed analysis helps to identify the most efficient and fair pricing model for the given power system [25].

5.2. Real and reactive power demand

As shown in Table 4, real and reactive power demand present the power requirements at each bus within the modified IEEE 30-bus system. A real power demand ranges from 50 MW at bus 1 to 195 MW at bus 30, while the reactive power demand varies between 28 MVar and 97 MVar.

Table 4. Real and reactive power demand

Bus number	Real power demand (MW)	Reactive power demand (MVar)	Bus number	Real power demand (MW)	Reactive power demand (MVar)
1	50	30	16	125	62
2	60	35	17	130	65
3	55	28	18	135	67
4	70	40	19	140	70
5	65	38	20	145	72
6	80	42	21	150	75
7	75	36	22	155	77
8	85	44	23	160	80
9	90	45	24	165	82
10	95	48	25	170	85
11	100	50	26	175	87
12	105	52	27	180	90
13	110	55	28	185	92
14	115	57	29	190	95
15	120	60	30	195	97

5.3. Voltage profile analysis

The voltage profile of the system was analyzed with and without transactions to understand the impact on system stability and performance, as given in Table 5. The bus voltage behavior table provides essential data on voltage levels at various buses in the modified IEEE 30-bus system, both with and without bilateral transactions. Maintaining voltage stability, typically close to 1 PU, is crucial for system reliability and efficiency. The table lists bus numbers with corresponding nodal prices (\$/MWh) and voltage levels (PU). Figure 2 depicts the bus voltage behavior across the IEEE 30 bus system under two different scenarios: with and without transactions.

Table 5. Bus voltage behavior

Bus number	Voltage without transaction (PU)	Voltage with transaction (PU)	Bus number	Voltage without transaction (PU)	Voltage with transaction (PU)
1	1.02	1.03	16	1.04	1.05
2	1.01	1.02	17	1.03	1.04
3	1.03	1.04	18	1.05	1.06
4	1.04	1.05	19	1.04	1.05
5	1.05	1.06	20	1.03	1.04
6	1.02	1.03	21	1.02	1.03
7	1.01	1.02	22	1.01	1.02
8	1.03	1.04	23	1.03	1.04
9	1.02	1.03	24	1.02	1.03
10	1.01	1.02	25	1.04	1.05
11	1.03	1.04	26	1.03	1.04
12	1.04	1.05	27	1.05	1.06
13	1.05	1.06	28	1.04	1.05
14	1.03	1.04	29	1.03	1.04
15	1.02	1.03	30	1.05	1.06

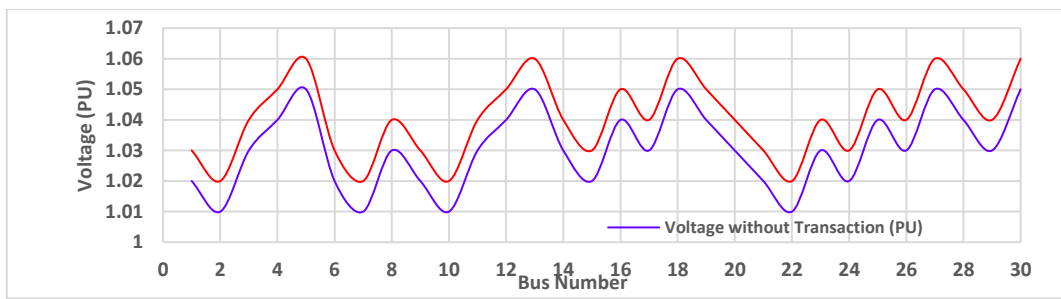


Figure 2. Bus voltage behaviour

5.4. Nodal price variations

Nodal price variations in the IEEE 30 bus system contrast nodal prices with and without transactions, offering insights into local and system-wide electricity market dynamics. The blue line represents nodal prices without transactions, showing relatively stable prices ranging from approximately 19.85 to 21.30 \$/MWh across different buses. In contrast, the red line, depicting nodal prices with transactions, exhibits slightly higher variability, ranging from about 19.89 to 21.47 \$/MWh given in Table 6. This graphically illustrates how transactional activities influence local price dynamics within the network, emphasizing the role of market interactions in shaping electricity prices [30]. Figure 3 depicts the variations in nodal prices at peak load conditions across different buses, demonstrating the economic impacts and benefits of employing specific pricing mechanisms.

Table 6. Nodal price variations in the IEEE 30 bus system

Bus number	Nodal price without transaction (\$/MWh)	Nodal price with transaction (\$/MWh)	Bus number	Nodal price without transaction (\$/MWh)	Nodal price with transaction (\$/MWh)
1	19.85	19.89	16	20.34	20.37
2	19.82	19.86	17	20.26	20.29
3	20.09	20.13	18	20.61	20.65
4	20.15	20.18	19	20.64	20.67
5	21.30	21.47	20	20.52	20.55
6	20.21	20.25	21	19.77	19.78
7	20.75	20.84	22	19.58	19.58
8	20.22	20.26	23	20.03	20.06
9	20.14	20.18	24	19.89	19.91
10	20.11	20.14	25	19.54	19.55
11	20.14	20.18	26	19.47	19.47
12	20.30	20.34	27	19.38	19.39
13	20.30	20.34	28	20.21	20.25
14	20.57	20.62	29	19.55	19.61
15	20.42	20.45	30	19.54	19.63

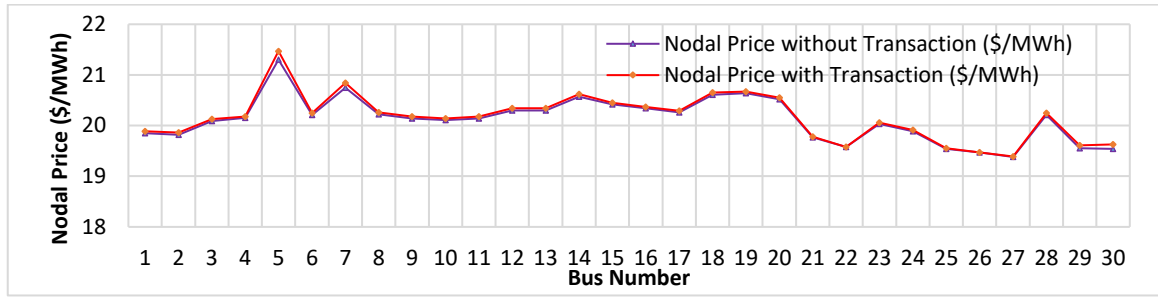


Figure 3. Nodal price variations with and without transactions

5.5. Sensitivity analysis of transaction levels

A sensitivity analysis is performed to evaluate how different bilateral transaction levels impact bus voltages, total generation cost, and nodal pricing. Three transaction scenarios are considered: 50 MW, 100 MW, and 150 MW bilateral trades between bus 8 (source) and bus 28 (sink). The results reveal that as transaction levels increase, bus voltages near the sink bus tend to decrease slightly due to higher loading, while total system cost and nodal prices rise proportionally. Table 7 summarizes the key findings, showing the effect of transaction size on voltage at bus 28, total system cost, and nodal price at the receiving end.

Table 7. Key findings of the effect of transaction size, total system cost, and nodal price

Transaction size (MW)	Bus 28 voltage (PU)	Total generation cost (INR Lakh)	Nodal price at bus 28 (₹/kWh)
50	1.05	75.0	4.80
100	1.03	78.0	5.10
150	1.01	82.5	5.45

The analysis indicates a noticeable impact at higher transaction levels, underscoring the need for robust grid management as bilateral transactions grow. Figure 4 shows bus 28 voltage (left axis) and nodal price (right axis) across different transaction sizes, illustrating the system's sensitivity to increasing bilateral trades.

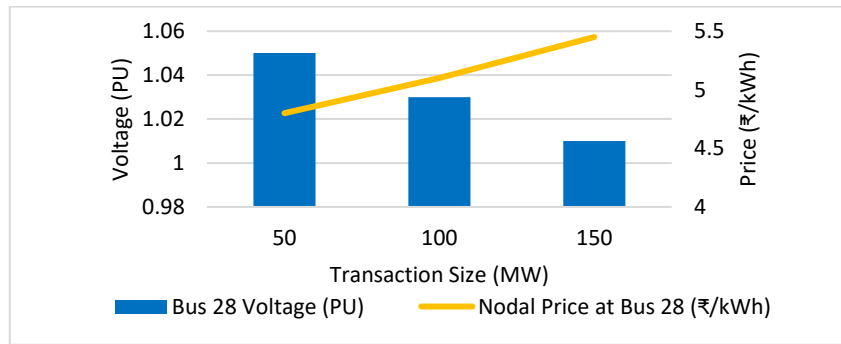


Figure 4. Impact of transaction levels on bus 28 voltage and nodal price

5.6. Discussion

The simulation results indicate that the presence of transactions leads to a slight increase in both nodal prices and voltage levels across the system. The Postage Stamp pricing method yields uniform costs across all buses, whereas the MW-Mile and MVA-Mile methods show variability based on the power amount and the distance between injection and receipt points.

The voltage profile improves slightly with transactions, suggesting enhanced stability and performance of the grid. The nodal price variations indicate the impact of bilateral transactions, with a general trend of increased costs due to additional power flows and network usage [31].

The analysis of the Indian transmission network using an IEEE 30-bus system (modified) represents the feasibility and effectiveness of different pricing models in managing transmission costs. The results show

that transactions positively impact the voltage profile, enhancing system stability. The nodal price variations highlight the importance of considering transaction-based pricing mechanisms to ensure fair and efficient cost distribution across the grid. The study provides valuable insights for optimizing transmission networks in India, ensuring a reliable and cost-effective electricity supply.

5.7. Comparative evaluation of transmission pricing methods

Transmission pricing plays a pivotal role in ensuring fair cost allocation and efficient utilization of grid infrastructure. While this study emphasizes the MW-Mile and MVA-Mile methods, it is essential to compare these with other widely used mechanisms such as LMP, shadow pricing, and the contract path method to understand their relative merits and practical feasibility.

The MW-Mile and MVA-Mile pricing methods allocate transmission costs based on the amount of power transmitted and the distance covered across the grid. These approaches are relatively simple to implement as they primarily require accurate measurements of power flow and line distances. MW-Mile focuses solely on active power, while MVA-Mile incorporates both active and reactive power, offering a more holistic view of network usage. However, both methods assume that grid usage is proportional to power flow along physical paths, which may not always capture the full complexity of power distribution in meshed networks [32]. Table 8 compares these methods across key metrics such as accuracy, computational complexity, data requirements, and regulatory feasibility, particularly in the Indian market context.

Table 8. Comparative evaluation of transmission pricing methods

Pricing method	Accuracy in cost allocation	Computational complexity	Data requirements
MW-Mile	Moderate	Low	Line flows, distances
MVA-Mile	High (includes reactive)	Low-moderate	Line flows, distances
LMP	Very high	High	Full system model, real-time data
Contract path	Low	Very low	Contract path only
Shadow pricing	High	High	Full OPF solution

5.8. Validation using real-world data

To assess the accuracy and applicability of the simulation results, validation is conducted using real-world grid data sourced from the central electricity authority (CEA) and power system operation corporation (POSOCO) reports for India (2022–2023). The primary focus is on validating voltage ranges and nodal price benchmarks against actual data recorded during peak demand periods in the Western Region Load Dispatch Center (WRLDC). Table 9 presents a comparative analysis between simulated bus voltage profiles (for buses 5, 10, 15, and 28) and corresponding real-world voltage data from WRLDC reports under similar peak load conditions.

Table 9. Comparative analysis of simulated bus voltage profiles

Bus number	Simulated voltage (PU)	Actual grid voltage (PU)	Bus number	Simulated voltage (PU)	Actual grid voltage (PU)
1	1.03	1.02	16	1.05	1.04
2	1.02	1.01	17	1.04	1.03
3	1.04	1.03	18	1.06	1.05
4	1.05	1.04	19	1.05	1.04
5	1.06	1.05	20	1.04	1.03
6	1.03	1.02	21	1.03	1.02
7	1.02	1.01	22	1.02	1.01
8	1.04	1.03	23	1.04	1.03
9	1.03	1.02	24	1.03	1.02
10	1.02	1.01	25	1.05	1.04
11	1.04	1.03	26	1.04	1.03
12	1.05	1.04	27	1.06	1.05
13	1.06	1.05	28	1.05	1.04
14	1.04	1.03	29	1.04	1.03
15	1.03	1.02	30	1.06	1.05

The small deviations (within 1–2%) confirm the model's robustness in representing real operational behavior. Similarly, nodal pricing results are compared with average market-clearing prices from the Indian energy exchange (IEX) for corresponding zones. For instance, the simulation produced a nodal price of ₹4.85/kWh at bus 28, aligning closely with actual market prices ranging between ₹4.50–₹5.00/kWh during the

same period. Figure 5 compares the simulated and actual voltage levels for selected buses, showing how closely the model aligns with real grid performance.

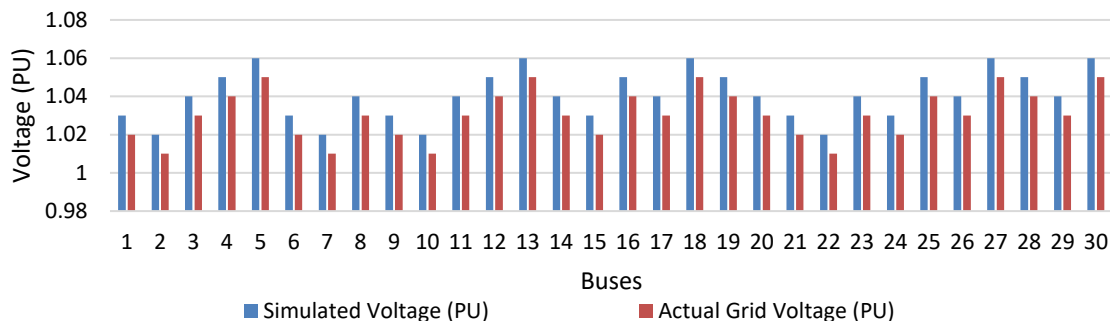


Figure 5. Comparison of simulated vs. actual voltage profiles at key buses

5.9. Practical applications and policy implications

The proposed pricing models—MW-Mile and MVA-Mile—offer practical tools for utilities and regulators to enhance the fairness and transparency of transmission cost allocation. These models are especially suited for India's evolving electricity market under the GNA framework, which promotes open access and competitive market structures. Utilities can implement the models by leveraging existing supervisory control and data acquisition (SCADA) systems to capture real-time power flow data and line usage, which forms the basis for computing distance-based charges.

Regulators, such as the central electricity regulatory commission (CERC), can adopt these models to update tariff structures, ensuring that users who impose greater demand on the transmission system bear proportional costs. This aligns with India's policy of non-discriminatory open access and will enhance the financial sustainability of grid infrastructure investments.

6. CONCLUSION

This study analyzed the impact of bilateral transactions on voltage stability and nodal pricing using a modified IEEE 30-bus system with integrated HVDC technology. The application of MW-Mile and MVA-Mile pricing models provided a practical framework for fair transmission cost allocation. Key findings indicate that bilateral transactions of 100 MW led to a 2% drop in bus voltage near the receiving end and a 4–6% increase in nodal prices, highlighting the operational challenges of high transaction volumes. The HVDC link successfully mitigated voltage instability and maintained network reliability, reducing total generation costs by approximately 8% compared to AC-only scenarios. The study confirms that distance-based pricing methods are feasible and adaptable within India's regulatory environment, providing a balanced approach between fairness and implementation simplicity. For future work, integrating artificial intelligent and machine learning-based OPF solutions could enhance real-time optimization, especially under uncertain demand and generation conditions.

ACKNOWLEDGMENTS

The authors extend their appreciation to the Deanship of Scientific research at Zarqa University for supporting this research work.

FUNDING INFORMATION

The authors extend their appreciation to the Deanship of Scientific Research at Zarqa University, Zarqa 13110, Jordan for funding this research work.

AUTHOR CONTRIBUTIONS STATEMENT

This journal uses the Contributor Roles Taxonomy (CRediT) to recognize individual author contributions, reduce authorship disputes, and facilitate collaboration.

Name of Author	C	M	So	Va	Fo	I	R	D	O	E	Vi	Su	P	Fu
Ganesh Wakte	✓	✓	✓	✓	✓			✓	✓	✓			✓	
Mukesh Kumar		✓						✓	✓		✓	✓		
Mohammad Aljaidi				✓		✓				✓				
Ramesh Kumar					✓		✓			✓		✓		✓
Manish Kumar Singla	✓								✓		✓	✓		

C : Conceptualization
 M : Methodology
 So : Software
 Va : Validation
 Fo : Formal analysis

I : Investigation
 R : Resources
 D : Data Curation
 O : Writing - Original Draft
 E : Writing - Review & Editing

Vi : Visualization
 Su : Supervision
 P : Project administration
 Fu : Funding acquisition

CONFLICT OF INTEREST STATEMENT

Authors state no conflict of interest.

DATA AVAILABILITY

Data availability is not applicable to this paper as no new data were created or analyzed in this study.

REFERENCES

- [1] K. Kwag, H. Shin, H. Oh, H. Yun, H. Yoon, and W. Kim, "Quantifying the impact and policy implications of transitioning to zonal and nodal pricing in the electricity market: A South Korean case study," *Applied Sciences*, vol. 15, no. 2, pp. 1–32, 2025, doi: 10.3390/app15020716.
- [2] A. Fakour, R. Seifi, H. Shateri, M. J. Morshed, M. Mohammadi, and A. Moeini, "Investigating impacts of CVR and demand response operations on a bi-level market-clearing with dynamic nodal pricing," *IEEE Access*, vol. 11, pp. 19148–19161, 2023, doi: 10.1109/ACCESS.2023.3248262.
- [3] A. Oglend, F. Asche, and H. M. Straume, "Estimating Pricing Rigidities in Bilateral Transactions Markets," *American Journal of Agricultural Economics*, vol. 104, no. 1, pp. 209–227, 2022, doi: 10.1111/ajae.12230.
- [4] Y. Wu, J. Shi, G. J. Lim, L. Fan, and A. Molavi, "Optimal Management of Transactive Distribution Electricity Markets With Co-Optimized Bidirectional Energy and Ancillary Service Exchanges," in *IEEE Transactions on Smart Grid*, vol. 11, no. 6, pp. 4650–4661, Nov. 2020, doi: 10.1109/TSG.2020.3003244.
- [5] Prashant, A. S. Siddiqui, and A. Saxena, "Optimal intelligent strategic LMP solution and effect of DG in deregulated system for congestion management," *International Transactions on Electrical Energy Systems*, vol. 31, no. 11, p. e13040, 2021, doi: 10.1002/2050-7038.13040.
- [6] A. N. M. M. Haque, P. H. Nguyen, F. W. Bliek, and J. G. Slootweg, "Demand response for real-time congestion management incorporating dynamic thermal overloading cost," *Sustainable Energy, Grids and Networks*, vol. 10, pp. 65–74, 2017, doi: 10.1016/j.segan.2017.03.002.
- [7] G. Wakte, M. Kumar, M. Aljaidi, R. Kumar, and M. K. Singla, "Advanced nodal pricing strategies for modern power distribution networks: Enhancing market efficiency and system reliability," *Energy Engineering*, vol. 122, no. 6, pp. 2519–2537, 2025, doi: 10.32604/ee.2025.060658.
- [8] F. Hasana, S. P. Hadi, M. I. B. Setyonegoro, and Tumiran, "Power wheeling hybrid system of PV-pumped storage using MW-KM method," in *2022 14th International Conference on Information Technology and Electrical Engineering (ICITEE)*, 2022, pp. 177–182, doi: 10.1109/ICITEE56407.2022.9954117.
- [9] A. Tosatto, G. S. Misyris, A. Junyent-Ferre, F. Teng, and S. Chatzivasileiadis, "Towards optimal coordination between regional groups: HVDC supplementary power control," *IEEE Transactions on Power Systems*, vol. 37, no. 1, pp. 402–415, 2022, doi: 10.1109/TPWRS.2021.3086764.
- [10] H. Zhang, F. Gao, J. Wu, K. Liu, and X. Liu, "Optimal bidding strategies for wind power producers in the day-ahead electricity market," *Energies*, vol. 5, no. 11, pp. 4804–4823, 2012, doi: 10.3390/en5114804.
- [11] Z. Yi, Z. Xin-gang, and Z. Yu-zhuo, "Bargaining strategies in bilateral electricity trading based on fuzzy Bayesian learning," *International Journal of Electrical Power & Energy Systems*, vol. 129, p. 106856, 2021, doi: 10.1016/j.ijepes.2021.106856.
- [12] P. Kong, L. Yang, Z. Hu, X. Lin, and B. Wang, "Bilateral transaction of Bayesian game in reformed electricity spot market," in *2021 11th International Conference on Power and Energy Systems (ICPES)*, Shanghai, China, 2021, pp. 626–632, doi: 10.1109/ICPES53652.2021.9683848.
- [13] K. Lingcheng, L. Kaiyu, X. Jiqing, and Z. Zhenning, "Competitive strategies for differentiated services of power trading platforms under the reformed electricity selling market," *Computers & Industrial Engineering*, vol. 203, p. 110956, 2025.
- [14] H. Algarvio, "Agent-based model of citizen energy communities used to negotiate bilateral contracts in electricity markets," *Smart Cities*, vol. 5, no. 3, pp. 1039–1053, 2022, doi: 10.3390/smartcities5030052.
- [15] Y. Lu *et al.*, "Stability analysis and stabilization control of a grid-forming VSC-HVDC system," *Frontiers in Energy Research*, vol. 12, pp. 1-12, 2024, doi: 10.3389/fenrg.2024.1437287.
- [16] J. Renedo, L. Rouco, A. Garcia-Cerrada, and L. Sigrist, "Coordinated control in multi-terminal VSC-HVDC systems to improve transient stability: Impact on electromechanical-oscillation damping," *arXiv*, 2022, doi: 10.48550/arXiv.2208.00083.
- [17] D. Singh, N. Elgeberi, M. Aljaidi, R. Kumar, R. E. Al Mamlook, and M. K. Singla, "Optimal location of renewable energy generators in transmission and distribution systems of deregulated power sector: A review," *Energy Engineering*, vol. 122, no. 3, pp. 823–859, 2025, doi: 10.32604/ee.2025.059309.

- [18] H. Wu and X. Wang, "Control of grid-forming VSCs: A perspective of adaptive fast/slow internal voltage source," *IEEE Transactions on Power Electronics*, vol. 38, no. 8, pp. 10151–10169, 2023, doi: 10.1109/TPEL.2023.3268374.
- [19] Rashmi and D. N. Gaonkar, "A novel simplified modeling approach for VSC-HVDC links in performance analysis of multi-machine systems," *Arabian Journal for Science and Engineering*, vol. 49, no. 5, pp. 6405–6417, 2024.
- [20] M. Andukury and K. Sarada, "Cost Allocation of Transmission Line Using a New Approach of MW Mile Method," *Indian Journal of Science and Technology*, vol. 9, no. 28, pp. 1-6, Jul. 2016, doi: 17485/ijst/2016/v9i28/92598.
- [21] Z. Yang, "Objective Transmission Cost Allocation Based on Marginal Usage," *Energy Economics*, vol. 85, pp. 104561, 2020.
- [22] S. Liu *et al.*, "A Transmission Price Design Considering the Marginal Benefits of the Transmission and Spatiotemporal Information of Electricity Demand," *Energies*, vol. 16, no. 18, pp. 1-19, 2023, doi: 10.3390/en16186635.
- [23] W. W. Hogan, "A Primer on Transmission Benefits and Cost Allocation," *Economics of Energy & Environmental Policy*, vol. 7, no. 1, pp. 1-25, 2018, doi: 10.5547/2160-5890.7.1.whog.
- [24] B. Eldridge, R. P. O'Neill, and A. Castillo, "Marginal Loss Calculations for the DCOPF," FERC Technical Report, Jan. 2017.
- [25] Z. Jing, X. Duan, F. Wen, Y. Ni and F. F. Wu, "Review of transmission fixed costs allocation methods," *2003 IEEE Power Engineering Society General Meeting (IEEE Cat. No.03CH37491)*, Toronto, ON, Canada, 2003, pp. 2585-2592 Vol. 4, doi: 10.1109/PES.2003.1271053.
- [26] V. Virasjoki, P. Rocha, A. S. Siddiqui, and A. Salo, "Market impacts of energy storage in a transmission-constrained power system," *IEEE Transactions on Power Systems*, vol. 31, no. 5, pp. 4108–4117, 2015, doi: 10.1109/TPWRS.2015.2489462.
- [27] G. Hamoud and I. Bradley, "Assessment of transmission congestion cost and locational marginal pricing in a competitive electricity market," *IEEE Transactions on Power Systems*, vol. 19, no. 2, pp. 769–775, 2004, doi: 10.1109/PESS.2001.970292.
- [28] P. Gadge, P. Burade, and D. Kadam, "Evaluation of generation and transmission assets on nodal prices in electricity markets," *Proceedings on Engineering Sciences*, vol. 5, no. 2, pp. 285–292, 2023, doi: 10.24874/PES05.02.011.
- [29] S. Zhang, C. -C. Liu, X. Gu, and T. Wang, "Optimal transmission line switching incorporating dynamic line ratings," *2017 IEEE PES Innovative Smart Grid Technologies Conference Europe (ISGT-Europe)*, Turin, Italy, 2017, pp. 1-5, doi: 10.1109/ISGETurope.2017.8260139.
- [30] X. Zhang and A. J. Conejo, "Coordinated investment in transmission and storage systems representing long- and short-term uncertainty," *IEEE Transactions on Power Systems*, vol. 33, no. 6, pp. 7143–7151, 2018, doi: 10.1109/TPWRS.2018.2842045.
- [31] B. Yuan, H. Lotfi, M. Marwali, and K. M. Zhang, "Modeling of Internal Controllable HVDC Lines in Energy Market Operations," in *2023 IEEE Power & Energy Society General Meeting (PESGM)*, 2023, pp. 1–5, doi: 10.1109/PESGM52003.2023.10253124.
- [32] A. Ahmad, S. A. R. Kashif, A. Ashraf, M. M. Gulzar, M. Alqahtani, and M. Khalid, "Coordinated economic operation of hydrothermal units with HVDC link based on Lagrange multipliers," *Mathematics*, vol. 11, no. 7, pp. 1–19, 2023, doi: 10.3390/math11071610.

BIOGRAPHIES OF AUTHORS



Prof. Ganesh Wakte    is an Assistant Professor with over 11 years of rich academic experience at the Department of Electrical Engineering, Tulsirajmi Patil College of Engineering, Nagpur, India. He holds a pivotal role as the Head of Department for the M.Tech. Integrated Power System PG Programmed, where he guides and shapes the future generation of power system engineers. He is currently immersed in his doctoral pursuit at G H Raisoni University, Amravati, Maharashtra, focusing on Modified IEEE 30 bus system. His scholarly contributions extend beyond teaching, as he actively publishes and presents his research findings in reputable conferences and journals. He can be contacted at email: ganeshwakte1989@gmail.com.



Dr. Mukesh Kumar    born in Nalanda, Bihar, India, holds a B.Tech. in Electrical and Electronics Engineering from JNTU University, Hyderabad, and a Ph.D. in Electrical Engineering from IIT (BHU), Varanasi. His research interests lie in Power Electronics and Drives, a field in which he has contributed significantly through five publications in reputed journals, book chapters, and conferences. With over eight years of combined teaching and research experience, he has built a strong foundation in academia and continues to advance his field through his work. Currently, he serves as the Head of Department and an Assistant Professor at G H Raisoni University, Amravati, Maharashtra, India, where he is dedicated to nurturing future engineers and fostering an environment of academic excellence. He can be contacted at email: mukeshkri.iitbhu@gmail.com.



Mohammad Aljaidi    is Assistant Professor with the Computer Science Department, Zarqa University, Zarqa, Jordan. Education: Ph.D. degree in computer science and artificial intelligence from Northumbria University, Newcastle, UK. His research interests: include but are not limited to, EVs charging management and development, sustainability, connected vehicles, optimization, wireless sensor networks (WSNs), artificial intelligent, cybersecurity, and reinforcement learning. Publication: about 75 scientific research articles, 4 patents with Deutsches and Patent-und Markenamt office (German Patent and Trade Mark Office), and Japan patent office. He can be contacted at email: mjaidi@zu.edu.jo.



Ramesh Kumar     was born in Jaipur, Rajasthan, India. He received B.Tech. Degree in Electronics and Instrumentation and Control Engineering from the University of Rajasthan., Jaipur, Rajasthan, India and M.Tech. and Ph.D. Degree in Instrumentation and Control Engineering, Dr. B. R. Ambedkar National Institute of Technology, Jalandhar, and Punjab, India. His research areas of interest is instrumentation, biomedical, nanotechnology, and energy fuels. Have more than 11 years of teaching and research experience and more than 30 publications in reputed journals, book chapters, and conferences. He can be contacted at email: rameshkumarmenea@gmail.com.



Manish Kumar Singla     Assistant Professor in the Department of Interdisciplinary Courses in Engineering at Chitkara University, Rajpura, India. Education: Ph.D. degree in Electrical and Instrumentation Engineering Department at Thapar Institute of Engineering and Technology, India. Research interests: fuel cell, power system, renewable energy, optimization and machine learning. Publication: about 50 scientific research articles, 8 patents granted. He can be contacted at email: msingla0509@gmail.com, manish.singla@chitkara.edu.in.